The Chemoenzymatic Synthesis of a Novel CBABC-Type Pentablock Copolymer and Its Self-Assembled "Crew-Cut" Aggregation

Ke Sha,[†] Dongshuang Li,[‡] Yapeng Li,[†] Bao Zhang,[†] and Jingyuan Wang*,[†]

Alan G. MacDiarmid Institute of Jilin University, No. 2519 Jiefang Road, Changchun 130023, P.R.China, and Research Institute of Tsinghua University in Shenzhen, No 7 GaoXinNan Road, Shenzhen, 518057, P.R. China

Received March 25, 2007; Revised Manuscript Received June 29, 2007

ABSTRACT: A symmetric linear CBABC pentablock copolymer consisting of poly(ethylene oxide) (PEO), polycaprolactone (PCL), and polystyrene (PSt) was synthesized by the combination of enzymatic ring-opening polymerization (eROP) and atom transfer radical polymerization (ATRP). Dihydroxyl-capped PEO first initiated eROP of ϵ-CL in the presence of biocatalyst Novozyme 435. Subsequently, the resulting dihydroxyl-terminated copolymer PCL-*b*-PEO-*b*-PCL was converted to bromine-ended triblock macroinitiator by the esterification with α-bromopropionyl bromide. Pentablock copolymer PSt-*b*-PCL-*b*-PEO-*b*-PCL-*b*-PSt was obtained via a subsequent ATRP of styrene(St), and its kinetics analysis indicated a "living"/controlled radical polymerization. The self-assembly behavior of pentablock copolymer was investigated in aqueous media. The "crew-cut" aggregates of various morphologies were observed, such as normal spherical micelles, rodlike micelles, vesicles, lamellae, and large compound micelles (LCMs). In addition, it was found that both the copolymer composition and the copolymer concentration in THF had a great influence on the morphologies of the aggregates.

Introduction

Biocatalyst enzyme has been used in a wide variety of polymerization reactions due to their high activity, nontoxicity, recyclability, and (enantio-, region-, and chemo-) selectivities while also being more environmentally friendly than some conventional organometallic catalysts. Enzyme-catalyzed polymerizations have been employed in the design and fabrication of various polyesters with different structures for increasing demands.[1,2] For example, immobilized enzyme Novozyme 435 has been recognized widely as an effective and versatile biocatalyst in polyester synthesis via both ring-opening polymerization (ROP) of lactones (e.g., ϵ-caprolactone)[3−5] and polycondensation of either diacid (its derivatives)/diol combinations[6−8] or hydroxyacids (its derivatives),[9,10] furthermore, its scope has been further widen by the preparation of block copolymers[11,12] and hyperbranched copolymers.[13] Consequently, the above merit of biocatalytic polymerization enables more attention concentrated on the development of mutually compatible chemo- and biocatalytic methods for wider applications.

Andreas Heise et al.[14] reported the first example of the chemoenzymatic synthesis of AB-type diblock copolymer PCL-*b*-PSt by combining eROP of CL and ATRP of St. Our groups also made use of this method to synthesize the triblock copolymer PSt-*b*-PCL-*b*-PSt[15] and functional amphiphilic epoxy-based diblock copolymer polycaprolactone-*block*-poly(glycidyl methacrylate).[16] However, this chemoenzymatic method has not been employed in the synthesis of symmetric quintuplet pentablock copolymers, which has been one of the challenges in polymer science not only for their rich morphological textures but also for their potential applications such as nanotechnology. As a matter of fact, there have been only a few publications on linear CBABC-type pentablock copolymers.[17−20] The traditional preparation of symmetric pentablock copolymers reported previously is mainly involved in two strategies: *Strategy I* relies on the sequential polymerization (e.g., two ATRP procedures[17] or two chemical ROP procedures[18]) of different monomer units from difunctional macroinitiator using the same polymerization system. *Strategy II* usually involves the coupling of the preformed polymer with functional groups at the chain ends.[19] Although these two strategies are effective and successful, it is difficult to address the issue of dissimilar monomer systems, which do not polymerize by the same chemistry.[20] It might require an intermediate transformation step to convert the end group of the preformed triblock copolymer (BAB) into an active initiating site for the polymerization of the second monomer (C). However, few reports are known about this strategy used for the preparation of pentablock copolymer.

In this paper, we concentrated on the chemoenzymatic synthesis of a novel amphiphilic CBABC-type pentablock copolymers based on PEO (block A), PCL (block B), and PSt (block C) by combining eROP and ATRP. The terminal hydroxyl function of PEO precursors was first employed in starting eROP of ϵ-CL in the presence of biocatalyst Novozyme 435. Subsequently, the resulting dihydroxyl-capped triblock copolymer HO-PCL-*b*-PEO-*b*-PCL-OH was activated with α-bromopropionyl bromide in order to initiate the ATRP of St. The synthetic route is illustrated in Scheme 1. The resulting pentablock copolymers PSt-*b*-PCL-*b*-PEO-*b*-PCL-*b*-PSt are especially interesting because PCL has features like crystallizability, lack of toxicity, printability, and good mechanical properties. On the other hand, the also crystallizable PEO has superior properties for being nontoxic, flexible, hydrophilic, weakly immunogenic, and biocompatible. In fact, the synthesis of a ternary ABC triblock copolymers based on PSt (block A), PEO (block B), and PCL (block C) has been reported.[21] Nevertheless, no reports have been published on analogous synthesis of linear symmetric pentablock copolymers using identical blocks. The aim of the research is to investigate further the compatibility among three different components as well as between eROP and ATRP.

* Corresponding author. E-mail: Jingyuanwang_jlu@yahoo.com.cn. Telephone/Fax: +86 431 5168216.
[†] MacDiarmid Institute of Jilin University.
[‡] Research Institute of Tsinghua University.

10.1021/ma0707234 CCC: $40.75
Published on Web 12/15/2007

Scheme 1. Synthesis of the Pentablock Copolymer PSt-*b*-PCL-*b*-PEG-*b*-PCL-*b*-PSt

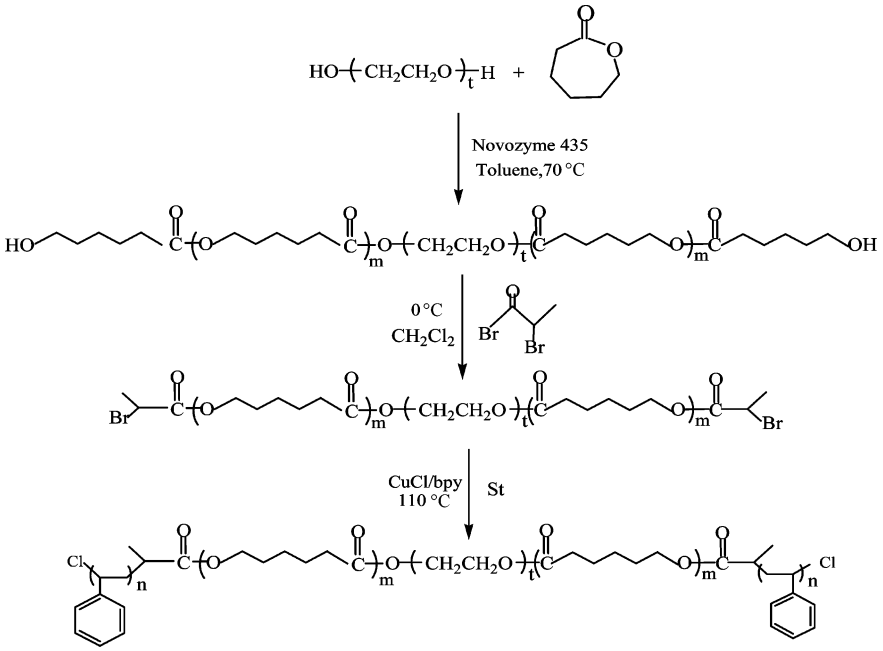

Table 1. Results for PCL-*b*-PEO-*b*-PCL 1, Macroinitiator Br-PCL-*b*-PEO-*b*-PCL-Br 2, and Its Pentablock Copolymers PSt-*b*-PCL-*b*-PEO-*b*-PCL-*b*-PSt 3−6

triblock copolymer	$[M]_o/[I]_o$	mol % carboxyl[a] terminal chains	monomer conv.[b]	$M_{n,th}$[c] (kg/mol)	$M_{n,nmr}$[a] (kg/mol)	$M_{n,GPC}$[d] (kg/mol)	M_w/M_n[d]
1	150/1	<2%	92%	19.8	19.3	16.1	1.38

macroinitiator	$[M]_o/[I]_o$	mol % the degree of[a] end functionalization	monomer conv.[b]	$M_{n,th}$[c] (kg/mol)	$M_{n,nmr}$[a] (kg/mol)	$M_{n,GPC}$[d] (kg/mol)	M_w/M_n[d]
2		>98%			19.9	16.8	1.36

pentablock copolymer	$[M]_o/[I]_o$	time (h)	monomer conv.[b]	$M_{n,th}$[c] (kg/mol)	$M_{n,nmr}$[a] (kg/mol)	$M_{n,GPC}$[d] (kg/mol)	M_w/M_n[d]
3	1000/1	2	4.8%	21.7	21.4	18.1	1.34
4	1000/1	4	10.3%	27.4	27.9	20.7	1.32
5	1000/1	12	27.5%	45.3	43.7	27.6	1.30
6	1000/1	24	53%	71.8	75.9	38.9	1.30

[a] Determined by NMR analysis. [b] The conversion was determined gravimetrically. [c] The theoretical molecular weights ($M_{n,th}$) calculated from the ratio of the initial monomer concentration to the initial initiator concentration $[M]_0/[I]_0$ and the monomer conversion. $M_{n,th} = ([M]_0/[I]_0)M_{monomer}\text{con.}\% + M_{n,macroinitiator}$ (1). [d] Determined by GPC measurements.

Because of the industrial and scientific significance, increasing interest has been arising on the "crew-cut" aggregates of block copolymer amphiphiles in selective solvents. The preliminary reports have described the preparation and observation of "crew-cut" aggregates of various morphologies from highly asymmetric diblock copolymer such as PSt-*b*-PEO[22−25] and polystyrene-*block*-poly(acrylic acid).[26−28] The morphologies include normal spheres, rods, lamella, vesicles, nanotubules, and large compound micelles (LCMs), etc. Self-assembled aggregates of the asymmetric diblock copolymers usually have core−corona structures. However, there are no reports on the "crew-cut" aggregates of amphiphilic symmetric pentablock copolymers, whose aggregation will result in a core−shell−corona structure. This type of multicompartment aggregates is significant in nanotechnology[29,30] because it is able to mimic basic properties of natural systems (e.g., serum albumins). Its applications in medicine, pharmacy, biotechnology, and so forth seem to be possible, but the preparation and control of stable multicompartment micellar systems are still at the very beginning.

Our group makes first use of new designed and synthesized amphiphilic symmetric pentablock copolymers PSt-*b*-PCL-*b*-PEO-*b*-PCL-*b*-PSt to explore/carry out the multicompartment "crew-cut" aggregates. The method of preparation involves dissolution of the copolymer in a good solvent, such as THF, and the subsequent addition of a precipitant (i.e., water) to induce aggregation of the hydrophobic blocks. The micellar morphologies were influenced remarkably by changing the initial copolymer concentration in organic solvent as well as the copolymer compositions. To our knowledge, this is the first example of "crew-cut" aggregates of amphiphilic symmetric pentablock copolymers.

Experimental Section

Materials. Novozyme-435 (immobilized *Candida antarctica* lipase B, specific activity 7000 PLU/g) was provided by Novozymes (Denmark). Dihydroxyl PEO with molecular weight of 4000 g/mol was purchased from Fluka Chemical Co. and used after dried in vacuo at 80 °C for 24 h. ϵ-Caprolactone and styrene were obtained from Aldrich Chemical Co. and distilled over calcium

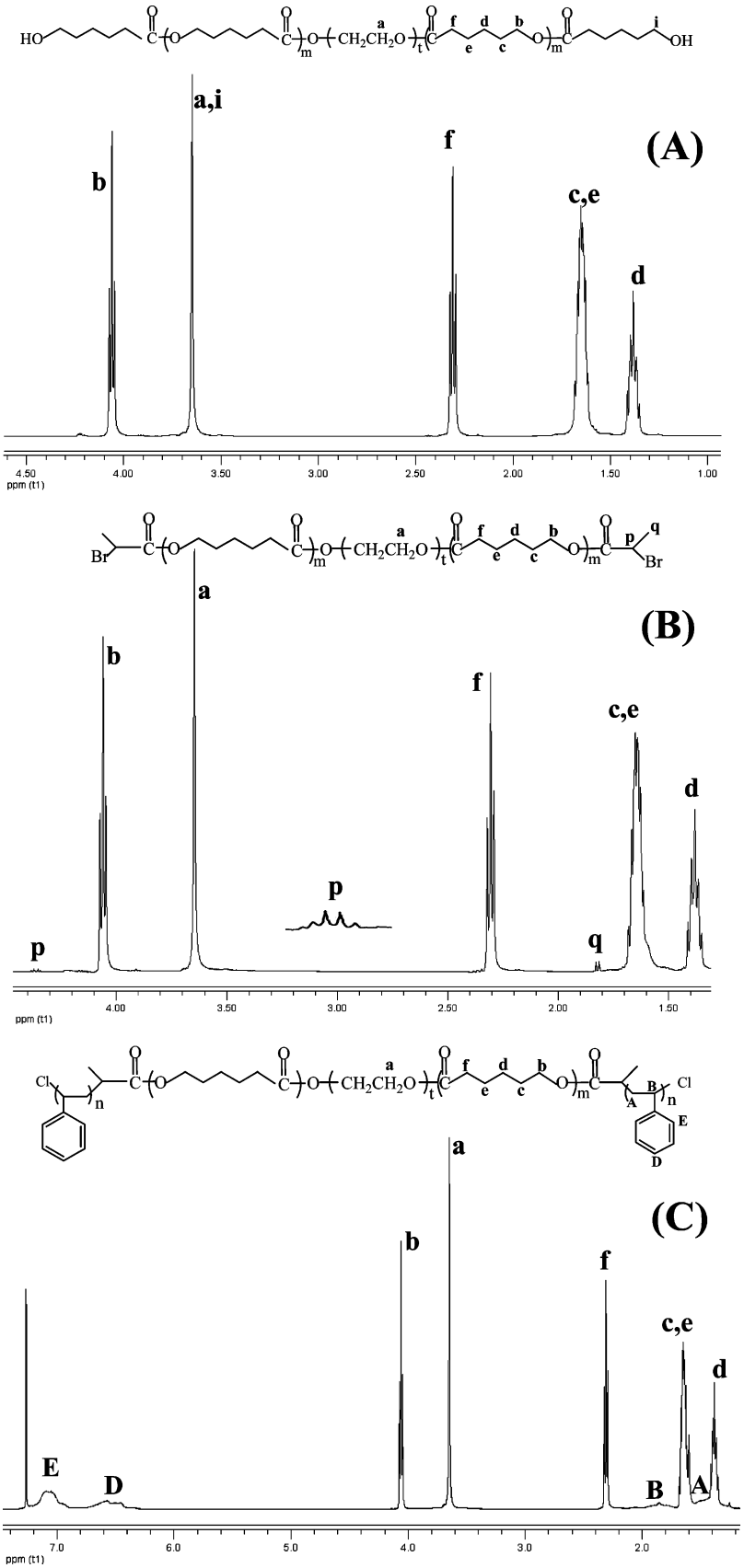

Figure 1. ^{1}H NMR ($CDCl_3$) spectra of (A) triblock copolymer **1** (1.93×10^4 g/mol, $M_{n,nmr} = (2I_{4.05}/I_{3.6-3.7})TM_{\epsilon-CL} + M_{PEO}$, $M_{\epsilon-CL}$ and M_{PEO} represents the molecular weight of ϵ-CL and PEO, respectively. T is the amount of the repeat units of PEO), (B) macrointiator **2** and (C) pentablock copolymers **4** (2.79×10^4g/mol, $M_{n,nmr} = (2I_{6.8-7.2}/I_{3.6-3.7})TM_{St} + M_{n,2}$, where M_{St} is the molecular weight of St and $M_{n,2}$ is GPC-determined M_n of **2**). $M_{n,nmr}$ was caculated from ^{1}H NMR integrated peak area I of peak n (I_n).

hydride (CaH_2) under vacuum before use. Copper(I) chloride (CuCl, Beijing Chemical Co.) was purified by precipitation from acetic acid to remove Cu^{2+}, filtrated and washed with ethanol, and then dried. 2,2′-Bipyridine (bpy, Beijing Chemical Co.) and α-bromopropionyl bromide (Fluka Chemical Co.) was used without further purification. Toluene (Tianjin Chemical Co.) and dichlo-

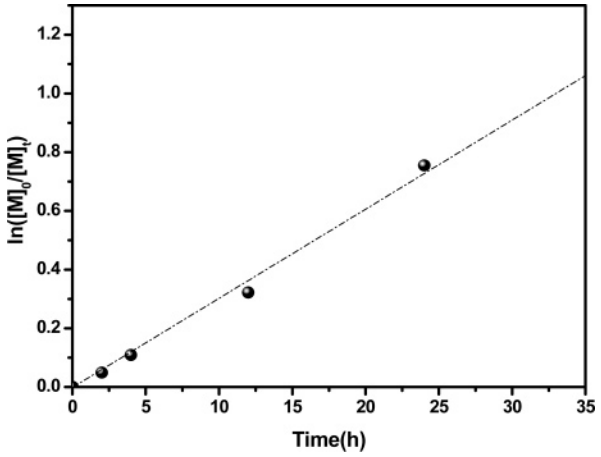

Figure 2. Relationship between $\ln([M]_0/[M]_t)$ and polymerization time for ATRP of St using macroinitiator **2**. $[M]_0$ and $[M]_t$ represent the initial monomer concentration and the monomer concentration after time *t*, respectively.

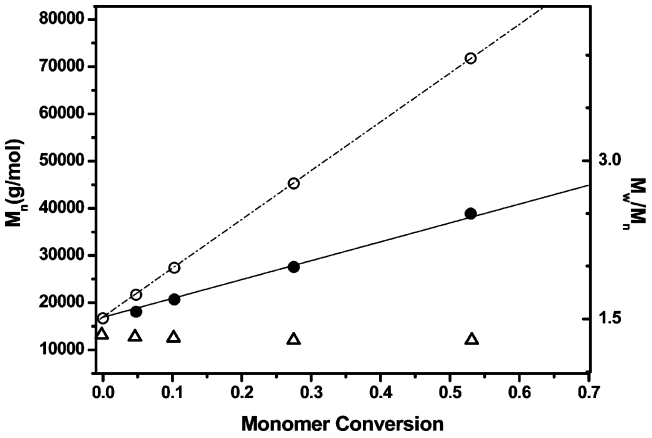

Figure 3. Dependence of M_n (●), $M_{n,th}$ (○) and polydispersity index (△) on monomer conversion for ATRP of St using macroinitiator **2**. The theoretical molecular weights ($M_{n,th}$) were calculated from eq 1 (Table 1).

romethane (CH_2Cl_2, Beijing Chemical Co.) were dried with CaH_2 and distilled under the protection of dry argon. Triethylamine (TEA, Beijing chemical Co.) was refluxed for 12 h in the presence of CaH_2 and distilled under vacuum. All the reagents used were of analytic grade.

Synthesis of Triblock Copolymer HO-PCL-*b*-PEO-*b*-PCL-OH. Novozyme-435 (0.216 g, 10% w/w of the monomer weight), dried over P_2O_5 in a vacuum desiccator (0.1 mmHg, 25 °C, 24 h), was transferred into an oven-dried 50 mL vial under an argon atmosphere. The monomer ϵ-caprolactone (2 mL, 18.9 mmol), the initiator dihydroxyl PEO (0.504 g, 0.126 mmol) and the solvent toluene (4.3 mL, twice v/w of the monomer) were added via syringe under argon into the reaction vial. The vial was then placed into a constant temperature (70 °C) oil bath with magnetic stirring for 4 h. Reactions were terminated by pouring into excess cold chloroform and removing the enzyme by filtration. The enzyme was washed several times with hot chloroform. The filtrate was concentrated by rotary evaporation. The crude products were dissolved in dichloromethane and precipitated at least in a 10-fold excess of methanol. Precipitation in methanol avoids the presence of residual monomer ϵ-CL. The final product was dried overnight in a vacuum oven. Yield: 1.739 g (80.7%).

Synthesis of Difunctional Triblock Macroinitiator Br-PCL-*b*-PEO-*b*-PCL-Br. The resulting HO-PCL-*b*-PEO-*b*-PCL-OH (1.0 g, 0.051 mmol) was dissolved in 5 mL of dry dichloromethane and then cooled in an ice bath (0 °C). Into this solution was added 0.07 mL (0.51 mmol) of TEA. After stirring for 5 min, 0.53 mL (0.51 mmol) of α-bromopropionyl bromide in 5 mL of dry

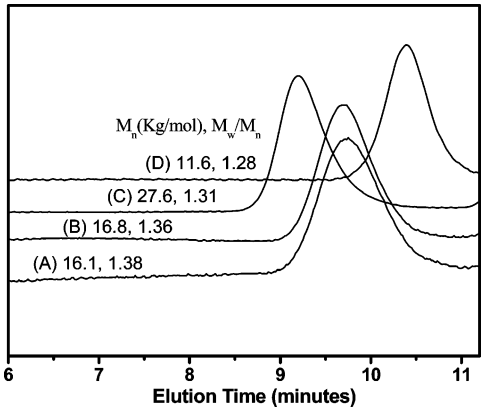

Figure 4. GPC traces of the triblock copolymer **1** (A), macrointiator **2** (B), the pentablock copolymers **5** (C), and its subsequent hydrolysate PSt (D). Molecular weight and polydispersity were determined by GPC calibrated with polystyrene.

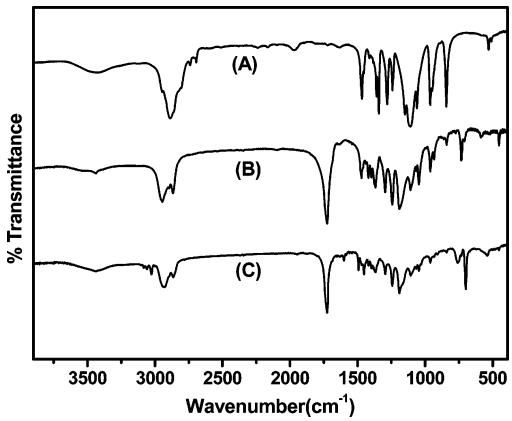

Figure 5. IR spectra of PEO4000 (A), PCL-PEO-PCL **1** (B) and its pentablock copolymer **5** (C).

dichloromethane was added dropwise to the solution over a period of 0.5 h. The reaction mixture was stirred at 0 °C for 2 h and then at room temperature for 22 h. The color of the solution changed from white to yellow. The precipitated byproduct was removed by filtration and then the filtrate was evaporated to dryness. The crude product was dissolved in 100 mL of dichloromethane, the organic phase was washed thoroughly successively with 5% aqueous $NaHCO_3$ and deionized water, and finally dried over $MgSO_4$. The concentrated solution was poured into methanol to precipitate the product. The resulting white solid was dried for 24 h in vacuo. Yield: 0.73 g (73%).

Synthesis of Pentablock Copolymer PSt-*b*-PCL-*b*-PEO-*b*-PCL-*b*-PSt. A dry flask equipped with a magnetic stirrer was charged with 0.008 g (0.08 mmol) of CuCl, 0.037 g (0.24 mmol) of bpy, and 0.3 g (0.015 mmol) of difunctional triblock macroinitiator. The reaction mixture was immersed in ice water/NaCl mixture at about −10 °C and degassed by vacuum-argon for three times, and then 1.73 mL (15 mmol) of monomer St and 1.73 mL (1/1 v/v of the monomer) of solvent toluene degassed by inert dry argon were introduced into the flask via a syringe under argon. After triblock macroinitiator was completely dissolved, polymerization was carried out under continuous stirring at a temperature of 110 °C for a predetermined time. Aliquots (about 0.3 mL of reaction mixture) were removed from the reaction mixture at selected time intervals to monitor the reaction progress. The conversion was determined gravimetrically after vacuum drying of the obtained aliquots. Finally, the reaction mixture was opened to air and cooled to room temperature. The catalyst was removed by passing the polymer solution through a short aluminum oxide column. The crude polymer was purified by precipitation in methanol and dried in a vacuum oven overnight.

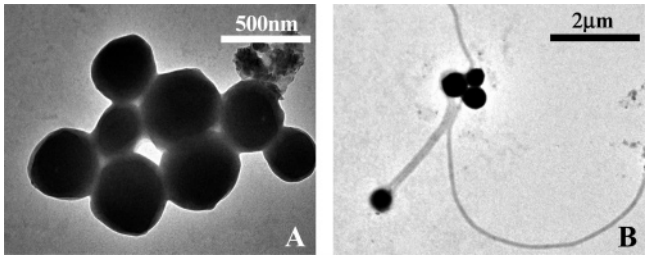

Figure 6. TEM pictures of LCMs from an aqueous solution of the pentablock copolymer **5**. The initial copolymer concentration in THF solvent was 3 mg/mL.

Hydrolysis of the Pentablock Copolymer. The PCL blocks were hydrolyzed by dissolving block copolymer (0.1 g) in a 10 mL mixture of 1,4-dioxane/hydrochloric acid (37%) (20:1 v/v). The mixture was then stirred for 24 h at 85 °C. After hydrolysis, the solvents were removed under vacuum, and the crude product was precipitated in cold methanol/H_2O (10:1 v/v). Yield: 0.03 g.

Formation of Copolymeric Micelles. The pentablock copolymer aggregates were prepared by the addition of water to copolymer solution in tetrahydrofuran (THF). Water is only good for the PEO block and is a precipitant for the other blocks, while THF is a common solvent for the PEO, PCL, and PSt block. First, the pentablock copolymers were stirred in distilled THF at different copolymer concentrations for 10 min at room temperature to obtain molecularly dispersed and homogeneous solution, and then distilled water was added dropwise into the copolymer solution with stirring to induce the micellization of the PCL and PSt blocks. As the water content in the solution increased, the solvent quality for the PCL and PSt block decreased. Usually, turbidity with a light-bluish tinge appeared, indicating the aggregation or micellization of the PCL and PSt block. The micelle solution was diluted to 20 mL with water and then sonicated for about 0.5 h at room temperature. A drop of the micelle solution of about 1 μL was dropped onto the silicon wafer surface/copper grids and dried in (vacuum) desiccator for the AFM/TEM analysis.

Characterization. The monomer conversion was determined gravimetrically. Measurements of nuclear magnetic resonance (NMR) spectra were conducted on a Bruker ARX-500 NMR spectrometer with $CDCl_3$ as solvent, operating at 500 and 125 MHz for the corresponding ^{1}H and ^{13}C nuclei, respectively. Chemical shifts (in ppm) were reported downfield using trimethylsilane as internal standard. Molecular weights and molecular weight distributions were measured on a Waters 410 gel permeation chromatography (GPC) apparatus equipped with a 10 μm Styragel HT6E column (300 mm × 7.8 mm) using linear polystyrene standards. THF was used as the eluent at a flow rate of 1 mL/min. The infrared spectra (IR) of polymers were recorded on a NICOLET Impact 410 at room temperature. Atomic force microscopy (AFM) observations of the micelles absorbed on the freshly treated silicon wafer surface[31] were carried out with the commercial instrument (Digital Instrument, Nanoscope IIIa, Multimode). All the tapping mode images were taken at room temperature in air with the microfabricated rectangle crystal silicon cantilevers (Nanosensor). The topography images were obtained at a resonance frequency of approximate 365 kHz for the probe oscillation. Transmission electron microscopy (TEM) studies were performed with a JEOL JEM 2010 instrument operated at an accelerator voltage of 200 KV. A drop of micelle solution was placed onto a carbon-coated copper grid. The excess sample was blotted off with filter paper. The samples were air-dried before measurement.

Results and Discussions

The synthesis of polyester−polyether type block copolymers has been investigated widely. Different types of PEO/PCL copolymers, including AB and BAB block copolymers, have been prepared using either chemo- or enzyme-catalyzed reactions.[11,32−34] Enzymatic synthesis of PEO/PCL diblock and triblock copolymers was first carried out by Zhou et al. in toluene using Novozyme-435 as catalyst.[11] Our group also used the same strategy for the preparation of triblock copolymer PCL-*b*-PEO-*b*-PCL **1** (Table 1) initiated with telechelic dihydroxyl PEO under anhydrous conditions.

A typical ^{1}H NMR spectrum of the resulting copolymer **1** was shown in Figure 1A. Besides the dominant PCL signals b−f, the sharp singlet peak a, corresponding to the methylene protons of initiator PEO, could be pointed out clearly at 3.67 ppm, which clarified PEO initiated eROP of ϵ-CL. In addition, the absence of a ^{13}C NMR signal at 177 ppm, corresponding to the carbon atom of the terminal carboxylic acid, suggested that the mole percentage of water-initiated PCL can be reduced to less than 2% (the limitation of detection by NMR analysis). At the same time, the GPC analysis of **1** showed a unimodal and symmetrical trace in Figure 4A. These results indicated quantitative initiation of PEO and the formation of triblock copolymers **1**. On the basis of the GPC measurement of the product, the NMR analysis, and the mechanism of eROP, it was concluded that the resulting copolymers **1** were also telechelic, that is, the linear PCL-*b*-PEO-*b*-PCL copolymer capped with two hydroxyl end groups.

The telechelic triblock macroinitiator Br-PCL-*b*-PEO-*b*-PCL-Br **2** (Table 1) for ATRP was prepared by reacting copolymer **1** with α-bromopropionyl bromide. To avoid cleavage of the polymer chains, the reaction was carried out at 0 °C in dried CH_2Cl_2 in the presence of TEA. The catalyst TEA can absorb HBr from the solution to generate a precipitate of quaternary ammonium halide $(CH_3CH_2)_3NH^+Br^-$, which benefited the esterification. The chemical structure of the resulting macroinitiator **2** was characterized by ^{1}H NMR spectroscopy (Figure 2B). Two new signals p and q appearing at 4.36 and 1.80 ppm were assigned to the methyne protons and the methyl protons adjacent to the active bromide, respectively. The result illustrated that the α-bromoester groups were attached to the triblock copolymer chain ends. The peak area ratio of a, p, and q is 90:0.5:1.5, which confirmed the complete substitution of the terminal hydroxyl groups. Besides, a narrow symmetrical GPC signal for macroinitiator **2** was also observed in Figure 4B. Comparison of the GPC analysis of macroinitiator **2** to copolymer **1** showed that number-average molecular weight (M_n) increased, but the polydispersity (weight-average molecular weight/number-average molecular weight (M_w/M_n)) was lower. This could be due to inevitable fractionation of macroinitiator during precipitation after esterification. The precipitated macroinitiator **2** was subsequently used for α-bromoester-mediated St polymerization.

The ATRP of St from macroinitiator Br-PCL-*b*-PEO-*b*-PCL-Br **2** was carried out in toluene at 110 °C using CuCl/bpy as the catalyst system. To confirm that the copolymerization of St was a living process, its reaction kinetics was investigated in detail. Figure 2 showed a first-order kinetics plot for the polymerization of St wherein a linear relationship was observed, indicating that the concentration of active species remained relatively constant throughout the reaction. The evolution of the GPC-determined M_n, theoretical molecular weight ($M_{n,th}$), and polydispersity vs monomer conversion was demonstrated in Figure 3. The molecular weight increased linearly with conversion while the polydispersities were low, less than 1.35. All pentablock copolymer products in kinetics study displayed narrow and unimodal elution peaks, and moreover, there were no obvious shoulders and tailings in GPC traces, suggesting the high initiation efficiency. A typical GPC curve of the pentablock copolymer **5** (Table 1) was shown in Figure 4C.

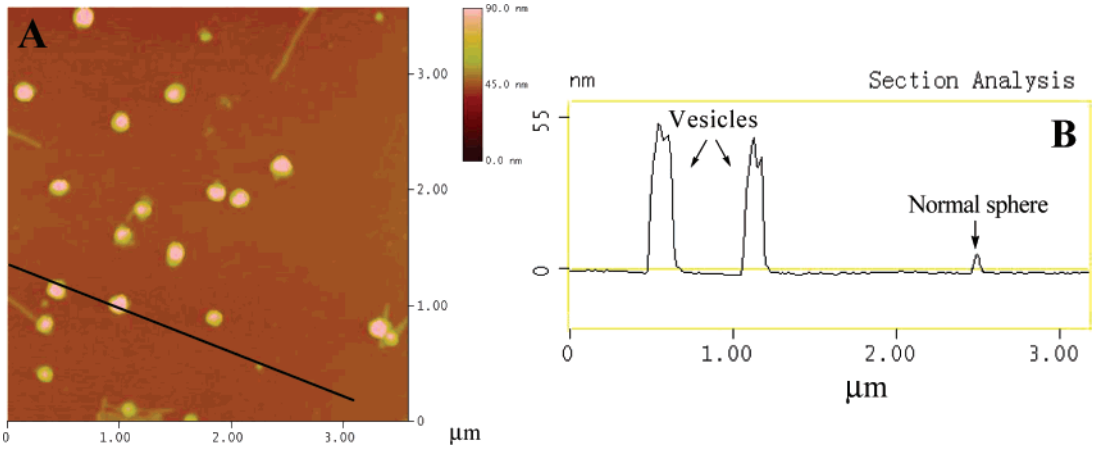

Figure 7. AFM height image (A) and cross-sectional analysis (B) of the aggregates from copolymer **5** *after exposure to high vacuum* at an initial copolymer concentration of 2 mg/mL. The cross-sectional profile B was measured along the solid line in image A.

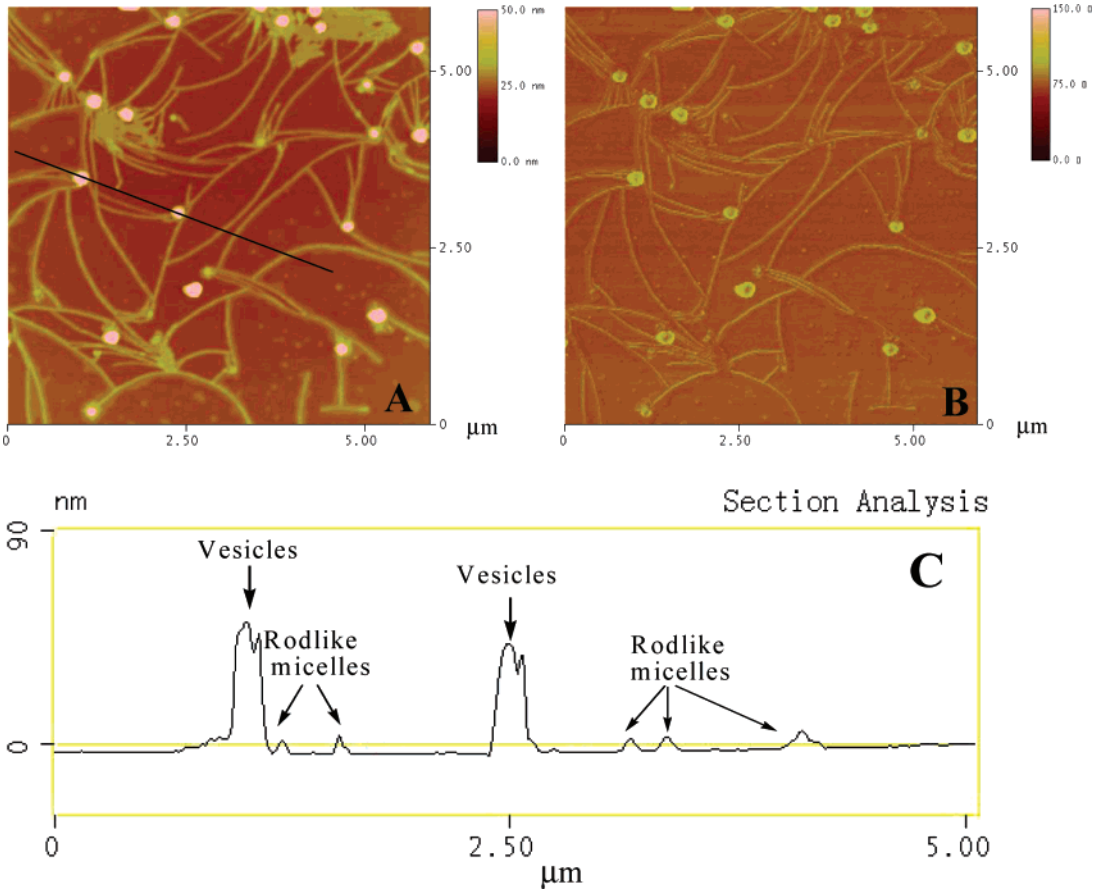

Figure 8. AFM height image (A), phase image (B), and cross-sectional analysis (C) of the rodlike micelles and vesicles from copolymer **5** *after exposure to high vacuum* at an initial copolymer concentration of 1 mg/mL.

The $M_{n,th}$ values were higher than the experimental ones (M_n), which resulted from the GPC technique underestimating M_n because of different hydrodynamic volumes of the copolymers and the linear polystyrene standards. Obviously, the kinetics behavior of ATRP indicated that the polymerization of St initiated with macroinitiator **2** was a "living"/controlled radical process.

Figure 1C showed a typical ^{1}H NMR spectrum of a pentablock copolymer. The resonance bands of the three blocks were clearly visible. In addition to the PEO peak a and the PCL signals b−f, the signals at 6.7−7.2 ppm were due to the aromatic protons D and E of the PSt block. Combing the GPC analysis (Figure 4), the NMR results indicated the formation of the pentablock copolymer PSt-*b*-PCL-*b*-PEO-*b*-PCL-*b*-PSt.

Figure 5 revealed the representative IR spectra of PEO, triblock copolymer PCL-*b*-PEO-*b*-PCL, and the related pentablock copolymer PSt-*b*-PCL-*b*-PEO-*b*-PCL-*b*-PSt. The ether stretch occurred at the wavenumbers of 1109 cm^{-1} for the PEO precursor (Figure 5A). After eROP of ϵ-CL, a new band occurred at 1734 cm^{-1} assigned to the carbonyl absorption of the PCL blocks (Figure 5B). With subsequent ATRP of St, all of the characteristic absorptions of PEO and PCL segments remained in the spectrum of pentablock copolymer (Figure 5C), at the same time, the new absorption peaks at about 3100, 1600, and 700 cm^{-1} illustrated the presence of PSt block. The variation in the IR spectra could be used as the indicative of successful preparation of the pentablock copolymer.

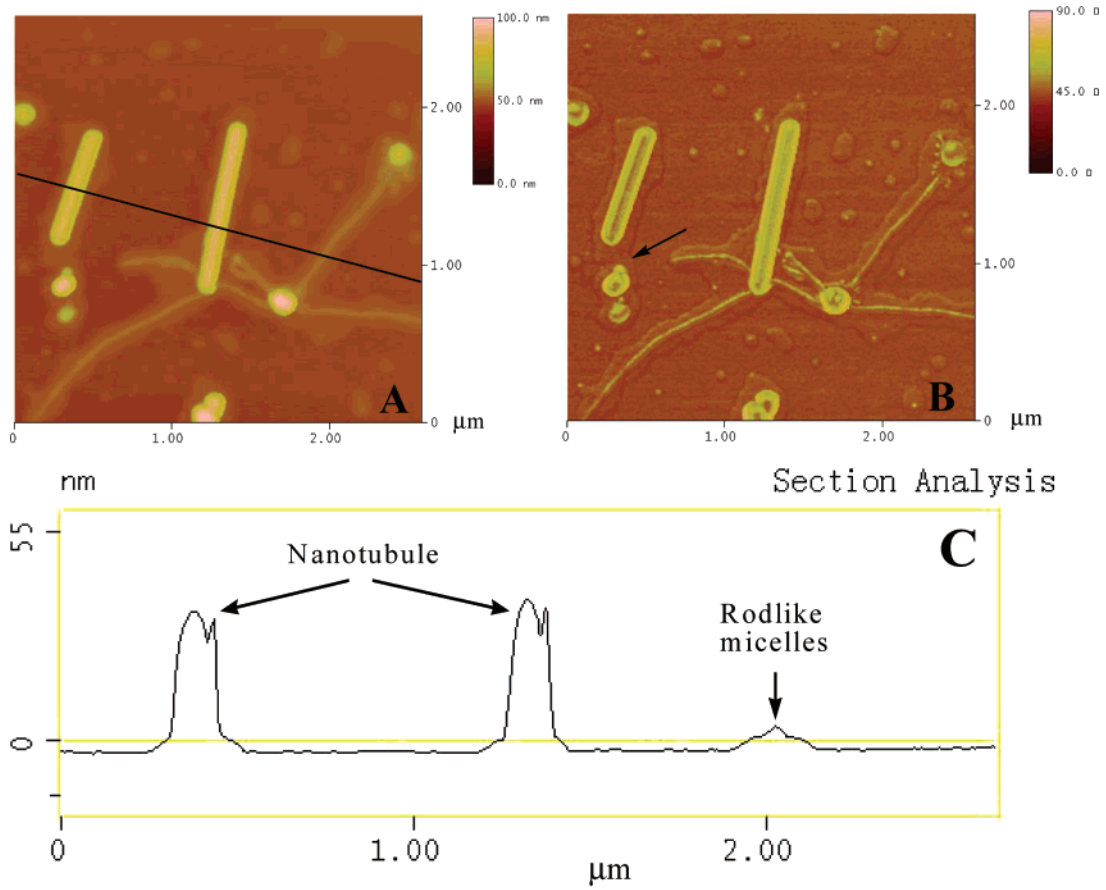

Figure 9. AFM height image (A), phase image (B), and cross-sectional analysis (C) of the nanoscale aggregates from copolymer **5** *after exposure to high vacuum* at an initial copolymer concentration of 1 mg/mL.

To further confirm the block copolymer structure, the pentablock copolymer **5** was dissolved in 1,4-dioxane and hydrolyzed with aqueous hydrochloric acid solution. The hydrolysis of the PCL segments bridged between PEO and PSt blocks resulted in the occurrence of the PEO and PSt homopolymer. PEO can be removed through precipitation in the mixture of methanol/water on the basis of its water solubility. Analysis of the resulting cleaved PSt by ^{1}H NMR and IR showed the disappearance of any PEO and PCL signals. Comparison of the GPC traces before and after hydrolysis was shown in Figure 4C,D, and it was observed that hydrolysis enabled a significant shift of the peak to lower M_n with low polydispersity.

In summary, NMR, IR, and GPC analysis proved that chemoenzymatic synthesis of pentablock copolymer PSt-*b*-PCL-*b*-PEO-*b*-PCL-*b*-PSt in two consecutive polymerizations, i.e., eROP and ATRP, was feasible and successful.

Eisenberg et al. first found and studied "crew-cut" aggregates of diblock copolymer PEO-*b*-PSt in aqueous solution.[22−25] As a novel system with different structures, analogical aggregates of multiple morphologies had also been observed in aqueous solution of pentablock copolymer PSt-*b*-PCL-*b*-PEO-*b*-PCL-*b*-PSt. To our knowledge, no study other than the present work focused on "crew-cut" pentablock copolymer aggregates. The preparation method involved copolymer dissolution in THF at room temperature, followed by the addition of water.

In previous reports where TEM was used as the normal technique to study "crew-cut" aggregates with various morphologies, it was crucial that TEM can detect the inner structure of the aggregaties; however, little attention was concentrated on tapping-mode AFM. In contrast to TEM analysis to determine the size and shape of the aggregates, AFM imaging was preponderant by the cross-sectional analysis, and it never required staining or coated by palladium/platinum alloy and thus reduced the possibility of the aggregate deformation. In addition, the inner structure of two hollow aggregates (i.e., vesicles and nanotubules) can also be validated according to the comparison of the AFM analysis before and after exposure to high vacuum.[35] Thus, our group made use of tapping-mode AFM as a predominant method, together with the necessary TEM analysis, to study the novel "crew-cut" pentablcok copolymer aggregates. In the AFM height images, the lateral dimensions of the aggregates were approximately taken as the diameter.

The morphologies were a function of both the copolymer composition and the copolymer concentration in the initial THF solution. The effect of the copolymer concentration in THF on the morphologies was studied first. The pentablock copolymers used in this study have the same PEO and PCL block length but different PSt block lengths; thus the effect of changes in the PSt block lengths on the morphologies was also investigated.

The aggregates of various morphologies were prepared from the pentablock copolymer **5** (Table 1) by changing the copolymer concentration in the initial THF solution. In most cases, aggregates of several different morphologies were seen in the same micrograph; only rarely were species of a single morphology observed. The variances of the morphologies observed were described below in order of decreasing copolymer concentration in the initial THF solution.

The 3 mg/mL copolymer concentration in the initial THF solution was first investigated, TEM analysis showed the pentablock copolymer **5** formed primarily large compound micelles (LCMs) with diameters varying from 200 to 800 nm in addition to small spheres with an average diameter of about

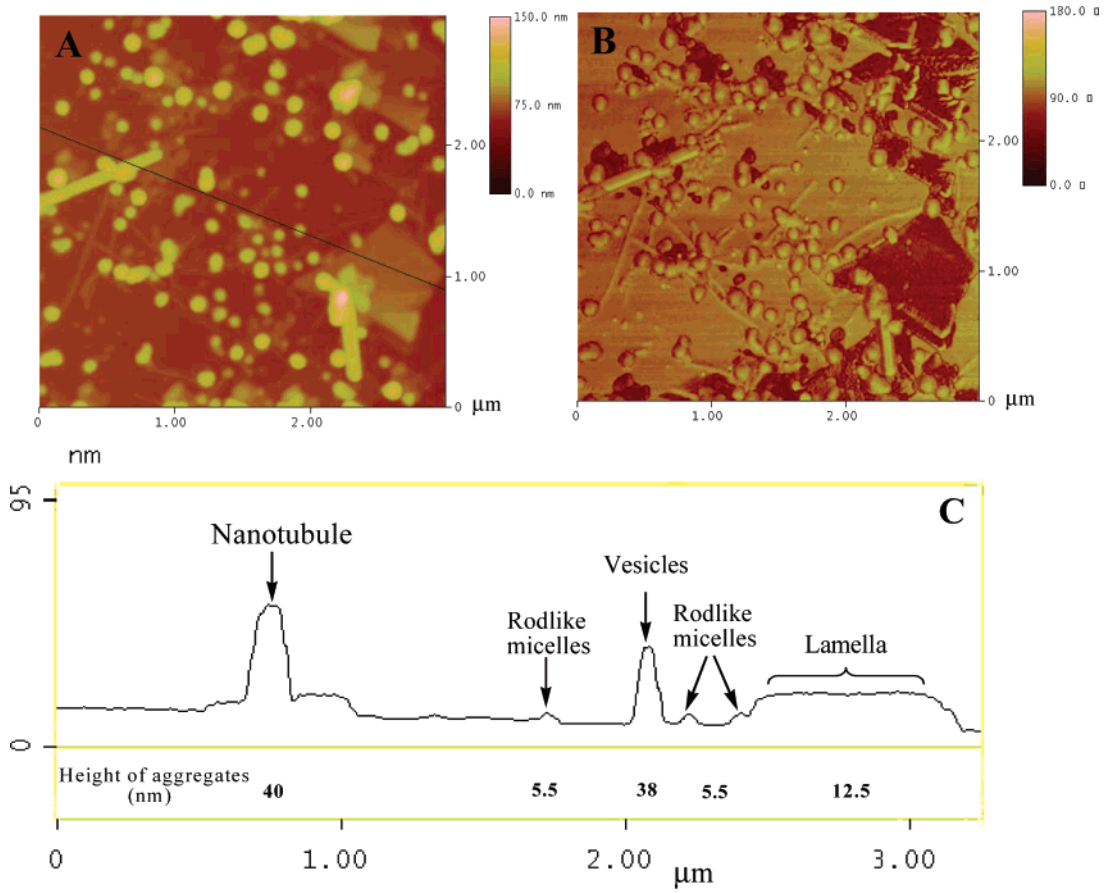

Figure 10. AFM height image (a), phase image (b) and cross-sectional analysis (C) of the various aggregates from copolymer **5** at an initial copolymer concentration of 0.5 mg/mL.

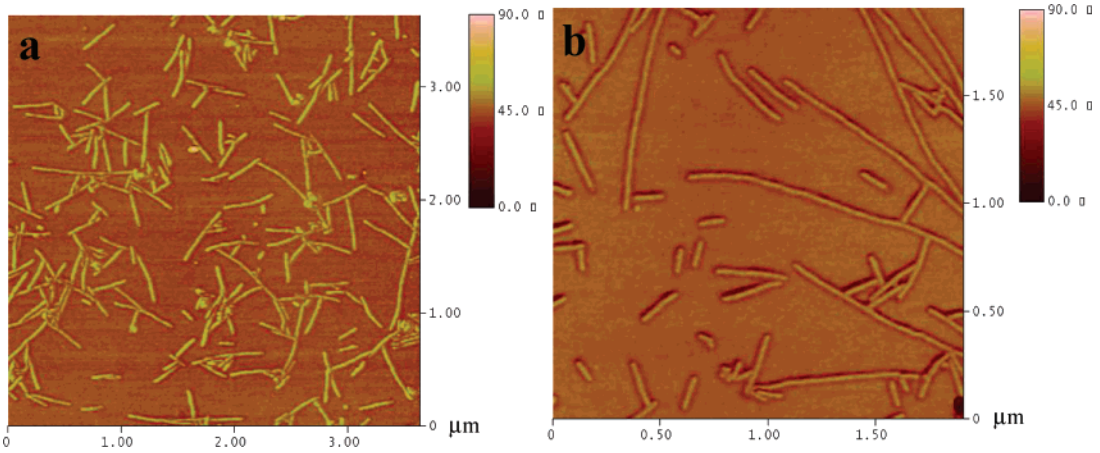

Figure 11. AFM phase images of the rodlike micelles from the pentablock copolymer **4** at different copolymer concentration in THF: (a) 3 mg/mL and (b) 2 mg/mL.

40 nm. A typical example of LCMs was shown in Figure 6A. LCMs with protruding rodlike micelles or nanotubules were also observed on some region of the micrograph (Figure 6B), however, they were few and encountered occasionally. The tubular nature is evident from the higher transmission in the central part of the aggregate compared to its periphery, indicating that the structure was hollow. The aggregates are obviously cylindrical from TEM images. The nanotubules had a uniform diameter of 180 nm, its lengths were very polydisperse, varying from hundreds of nanometers to several micrometers, but the wall thickness was quite uniform (about 60 nm). The rodlike micelles were about 100 nm in diameter and reached tens of micrometers in length.

Figure 7 showed a typical AFM image of the aggregates made from a 2.0 mg/mL copolymer **5** THF solution, where the sample was exposed to high vacuum. Obviously, two spherical species with different dimension were observed by cross-sectional analysis in Figure 7B. According to the previous reports,[22−25] it was concluded that the smaller spheres (very rarely) were the normal "crew-cut" micelles and had about 50 nm in average diameter, while the larger spheres (primarily) were believed to be vesicles with an average diameter of about 200 nm. Additional species such as rodlike micelles were encountered occasionally as minority morphology; the rodlike micelles had a diameter of about 90 nm, and the lengths were quite polydisperse and less than 600 nm.

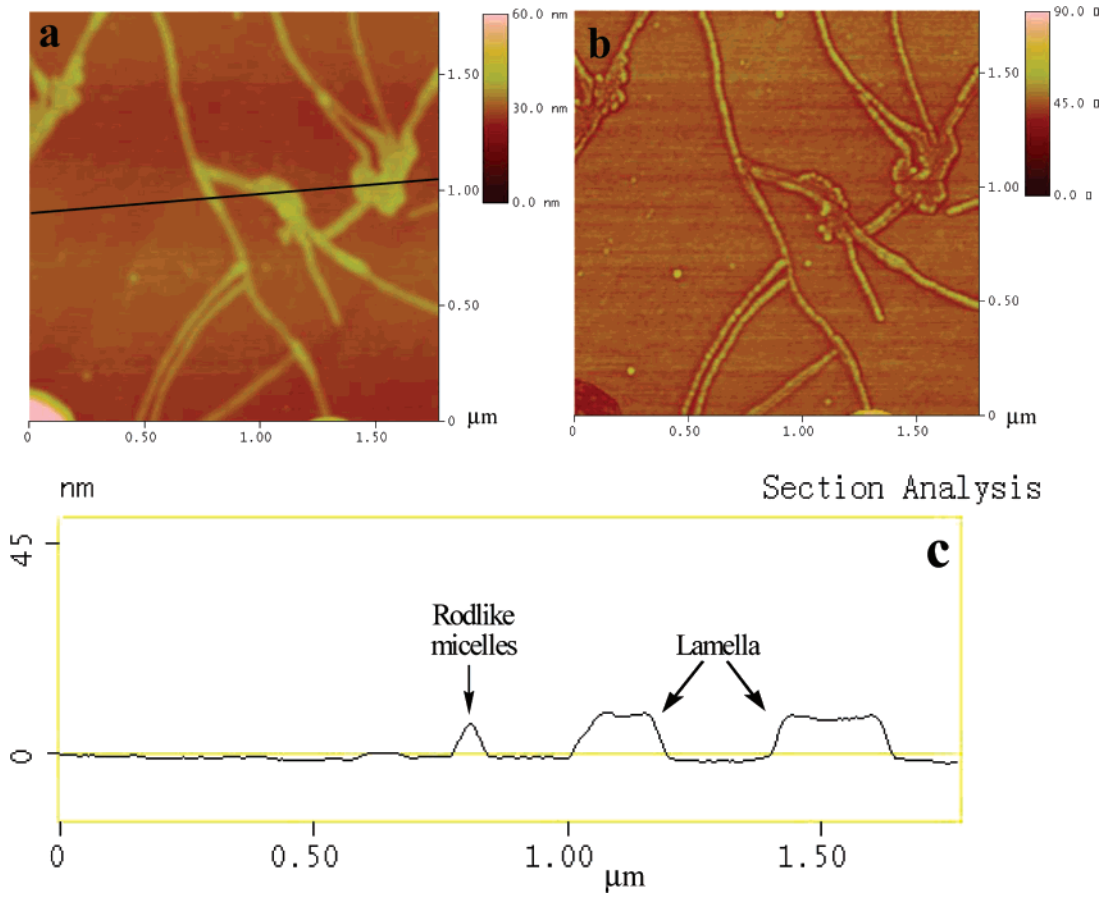

Figure 12. Tapping-mode AFM images of the aggregates formed from copolymer **4**: (a) height image, (b) phase image, and (c) cross-sectional analysis. The copolymer concentration in the initial THF solution was 1 mg/mL.

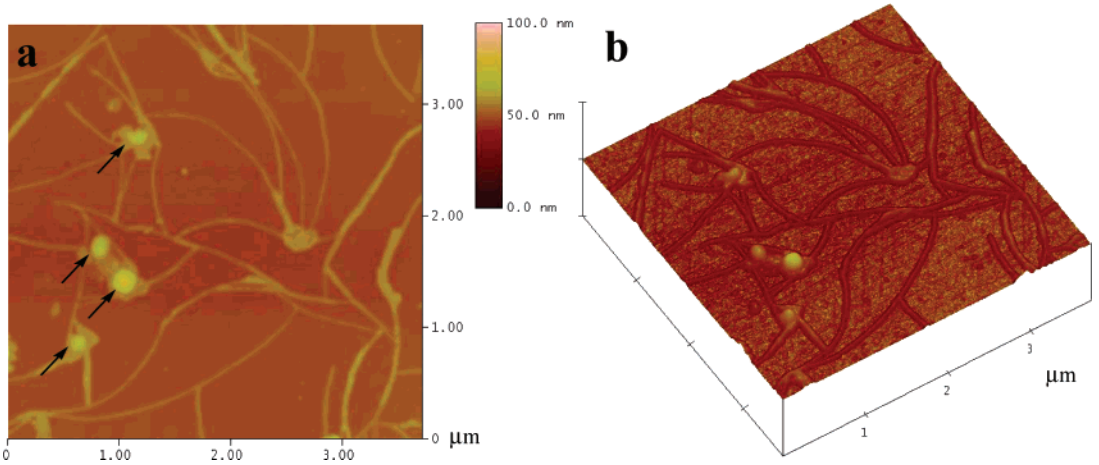

Figure 13. Tapping-mode AFM images of the unformed vesicles formed from copolymer **4**: (a) height image, (b) 3D image. The copolymer concentration in the initial THF solution was 1 mg/mL.

To collect the evidence for the hollow spherical vesicles, the same sample used previously for tapping-mode AFM was under high vacuum overnight. The second cross-sectional analysis showed that the vesicles had a collapsed center after exposure to high vacuum, as shown in Figure 7B. The diameter of the vesicles were the same before and after exposure to high vacuum; however, the height of vesicles decreased little, which indicated that no significant morphological changes occurred other than the collapse. At the same time, the shape and height of normal micelles and the rodlike micelles in the same sample remain invariable. Thus, the AFM analysis in Figure 7 provided the evidence that the structure of the larger spheres were hollow vesicles.

As the copolymer concentration in initial THF solution decreased to 1 mg/mL, as shown in Figure 8 and Figure 9, the sample formed primarily rodlike micelles with an admixture of vesicles and (rarely) nanotubules. A larger number of small normal micelles with a diameter of about 50 nm were also observed in AFM images. The rodlike micelles were about 90 nm in diameter and had a length from hundreds of nanometers to *two* or *three* micrometers. It was also observed that the rodlike micelles mostly were cross-linked. The end caps of cylinders had a spherical geometry. The energy cost of these spherical end caps become higher, thus it was favorable for the rodlike micelles to either form longer cylinders or carry out cross-linkage in order to reduce the number of end caps.[36]

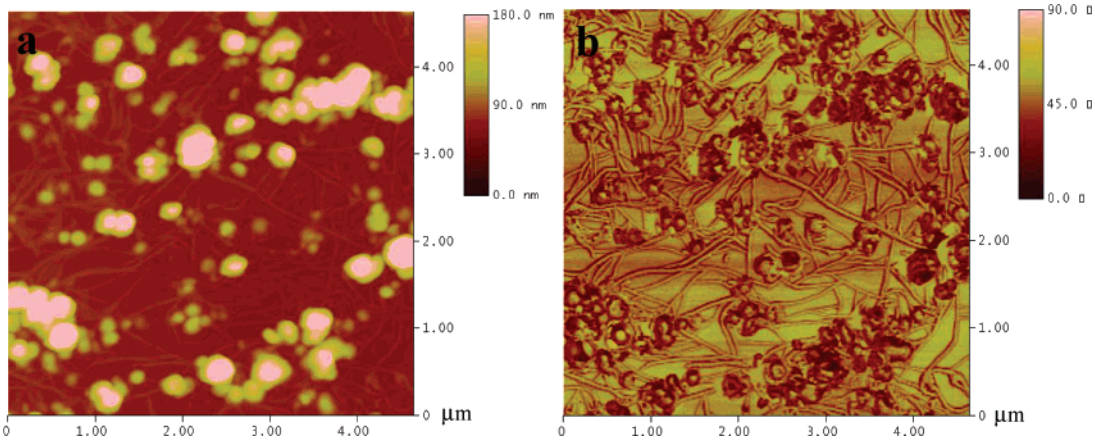

Figure 14. AFM height image (a) and phase image (b) of the rodlike micelles and vesicles from copolymer **4** at an initial copolymer concentration of 0.5 mg/mL.

Nanotubules with a collapsed center appeared in Figure 9 after exposure to high vacuum. The collapsed structures indicated further the nanotubules were hollow, as proved by TEM analysis (Figure 6). The diameter of the nanotubules from AFM analysis was 200 nm, consistent with that based on the TEM measurement (180 nm). As expected, the collapsed vesicles were also shown in Figure 8 by the cross-sectional analysis after exposure to high vacuum.

The nanotubules were closed cylinders with hemispherical terminals, as shown in Figure 9. Thus, nanotubules had a tendency for longer size based on the same reason as the rodlike micelles. A possible intermediate course, i.e., vesicles would be connected to the end of nanotubules (arrow), was taken by AFM measurement. This suggested that vesicles may be precursors of nanotubules.

Figure 10 shows an AFM micrograph of lamellar aggregates made from a 0.5 mg/mL copolymer solution in THF. The nature of the lamellar structure was evidenced by the uniform height over the overall part of the aggregates according to the cross-sectional analysis in Figure 10C. The cross-sectional profile demonstrated that the thickness of the lamella (12.5 nm) was approximately twice the height of the rodlike micelles (5.5 nm), which was consistent with the bilayer structure expected for the lamella.[36] The resulting lamellas were stable, with the characteristic wrinkles and wedgelike cuts. Lots of vesicles and nanotubules were also seen in addition to a small quantity of normal spherical micelles and rodlike micelles, however, the sizes of these four aggregates varied little in contrast to those obtained from higher copolymer concentrations in THF. In addition, it was observed in Figure 10C that no vesicles and nanotubules had a collapsed center when the sample was not exposed to high vacuum.

The effect of the PSt block length on morphologies was also investigated in brief. Pentablock copolymer **4** had the same length of PEO and PCL blocks as copolymer **5** but a shorter PSt block. Subsequently, we studied the aggregates of several different morphologies obtained from copolymer **4** wherein the variances of the copolymer **4** concentrations in initial THF solution were accordant with that of copolymer **5** for convenient comparison. The normal small spherical micelles with an average diameter of 30 nm appeared in each of the samples.

The copolymer **4** formed primarily rodlike micelles as the copolymer concentrations in THF were 3 and 2 mg/mL, shown in Figure 11 a and b, respectively. Comparison of the AFM images indicated that lower copolymer concentration resulted in longer rodlike aggregates, for example, the length of the rodlike micelles never exceeded 600 nm in Figure 11a, however, some rods reached 2000 nm in length in Figure 11b. Obviously, the diameter of two rodlike micelles remained invariance; both were about 50 nm.

As the copolymer concentration in THF decreased to 1 mg/mL, the AFM images of cross-linked rodlike micelles were presented in Figure 12. It had an average diameter of about 50 nm. Some aggregates with lamellar structure were also observed, evidenced by the uniformity of the height in Figure 12c. Its height (8 nm) was not twice that of rodlike micelles (5.5 nm); it was obvious that the lamellar structure was not bilayer. The lamella observed usually had protruding rodlike micelles attached to them. In some regions, the appearance of a few vesicles (including the unformed vesicles) over the lamellas (arrows in Figure 13a) indicated this type of lamella could be the precursors of large vesicles. This morphology does not represent equilibrium but probably involves a trapped intermediate structure. The conclusion was testified with the phenomenon that the vesicles almost appeared in the infall of rodlike micelles in Figures 8 and 14. Thus, this type of lamella was called an "intermediate lamella". Besides its height, the morphology of "intermediate lamella" in Figure 12 was very different from that of the lamella observed in Figure 10.

When the copolymer concentration in THF was 0.5 mg/mL, lots of vesicles were observed over the network from rodlike micelles in Figure 14.

The above information, together with the results of the preliminary reports,[22−25] showed that the morphologies of self-assembled aggregates were affected by the block copolymer composition as well as the copolymer concentration in the initial THF solution. The higher PSt content in pentablock copolymer and the lower copolymer concentration in THF enabled the change of the aggregates for the more stable morphologies from sphere to rod to bilayers (i. e., vesicles, nanotubules, and lamella). In general, LCMs, nanotubules, and lamella were only prepared from pentablock copolymer **5** with longer PSt blocks. Thus, the copolymer composition played a major role in determining the morphologies of the aggregates; however, the copolymer concentration in THF was also relevant.

Conclusions

The chemoenzymatic synthesis of a PSt-*b*-PCL-*b*-PEO-*b*-PCL-*b*-PSt pentablock copolymer, by a combination of eROP and ATRP, has been described. The kinetic study of ATRP demonstrated that the telechelic triblock macroinitiator Br-PCL-*b*-PEO-*b*-PCL-Br started effectively the polymerization of St, leading to a controlled PSt block. The structures of all the

polymer products have been well characterized by means of NMR, GPC, and IR measurement.

The "crew-cut" aggregates of various morphologies formed from pentablock copolymer in dilute aqueous solutions were observed by tapping-mode AFM and TEM. The morphologies were a function of the copolymer composition as well as, to a lesser extent, the block copolymer concentration in THF. The aggregate morphologies observed were co-incident with the aggregation phenomena of diblock copolymer PSt-*b*-PEO, except for lamellar aggregates. Two different lamellas (i.e., bilayer lamella and "intermediate" lamella) were observed, which will be investigated further and presented in a subsequent paper. In addition, experiments aiming to the effect of the solvent nature, temperature, and the storage time on the morphologies are under way.

Acknowledgment. We are grateful to the Natural Science Foundation of P. R. China for the support of this work (no. 20574028).

References and Notes

(1) Kobayashi, S.; Uyama, H.; Kimura, S. *Chem. Rev.* **2001**, *101*, 3793.
(2) Gross, R. A.; Kumar, A.; Kalra, B. *Chem. Rev.* **2001**, *101*, 2097.
(3) Uyama, H.; Suda, S.; Kikuchi, H.; Kobayashi, S. *Chem. Lett.* **1997**, 1109.
(4) Uyama, H.; Kobayashi, S. *Chem. Lett.* **1993**, 1149.
(5) Knani, D.; Gutman, A. L.; Kohn, D. H. *J. Polym. Sci., Part A: Polym. Chem.* **1993**, *31*, 1221.
(6) Mahapatro, A.; Kumar, A.; Kalra, B.; Gross, R. A. *Macromolecules* **2004**, *37*, 35.
(7) Mahapatro, A.; Kalra, B.; Kumar, A.; Gross, R. A. *Biomacromolecules* **2003**, *4*, 544.
(8) Wallace, J. S.; Morrow, C. J. *J. Polym. Sci., Part A: Polym. Chem.* **1989**, *27*, 3271.
(9) Mahapatro, A.; Kumar, A.; Gross, R. A. *Biomacromolecules* **2004**, *5*, 62.
(10) O'Hagan, D.; Zaidi, N. A. *Polymer* **1994**, *35*, 3576.
(11) He, F.; Li, S.; Vert, M.; Zhou, R. *Polymer* **2003**, *44*, 5145.
(12) Panova, A. A.; Kaplan, D. L. *Biotechnol. Bioeng.* **2003**, *84*, 103.
(13) Skaria, S.; Smet, M.; Frey, H. *Macromol. Rapid Commun.* **2002**, *23*, 292.
(14) Meyer, U.; Palmans, A. R. A.; Loontjens, T.; Heise, A. *Macromolecules* **2002**, *35*, 2873.
(15) Sha, K.; Qin, L.; Li, D.; Liu, X.; Wang. J. *Polym. Bull.* **2005**, *54*, 1.
(16) Sha, K.; Li, D.; Li, Y.; Liu, X.; Wang, S.; Guan, J.; Wang, J. *J. Polym. Sci., Part A: Polym. Chem.* **2007**, *45*, 5037.
(17) Darcos, V.; Haddleton, D. M. *Eur. Polym. J.* **2003**, *39*, 855.
(18) Ling, J.; Chen, W.; Shen, Z. *J. Polym. Sci., Part A: Polym. Chem.* **2005**, *43*, 1787.
(19) Thunemann, A. F.; Kubowicz, S.; von Berlepsch, H.; Mohwald, H. *Langmuir* **2006**, *22*, 2506.
(20) Toman, L.; Janata, M.; Sikora, A. *J Polym Sci., Part A: Polym Chem.* **2004**, *42*, 6098.
(21) Arnal, M. L.; Balsamo, V.; Lopez-Carrasquero, F.; Contreras, J.; Carrillo, M.; Schmalz, H.; Abetz, V.; Laredo, E.; Muller, A. J. *Macromolecules* **2001**, *34*, 7973.
(22) Yu, K.; Eisenberg, A. *Macromolecules* **1996**, *29*, 6359.
(23) Yu, K.; Eisenberg, A. *Macromolecules* **1998**, *31*, 3509.
(24) Yu, K.; Zhang, L.; Eisenberg, A. *Langmuir* **1996**, *12*, 5980.
(25) Yu, K.; Bartels, C.; Eisenberg, A. *Langmuir* **1999**, *15*, 7157.
(26) Zhang, L.; Eisenberg, A. *J. Am. Chem. Soc.* **1996**, *118*, 3168.
(27) Yu, Y.; Zhang, L.; Eisenberg, A. *Macromolecules* **1998**, *31*, 1144.
(28) Burke, S. E.; Eisenberg, A. *Langmuir* **2001**, *17*, 6705.
(29) Tu, R. S.; Tirrell, M. *Adv. Drug Delivery Rev.* **2004**, *56*, 1537.
(30) Lutz, J. F.; Laschewsky, A. *Macromol. Chem. Phys.* **2005**, *206*, 813.
(31) Treatment of silicon wafers: The silicon wafers were ultrasonically cleaned for 5 min in succession with toluene, acetone, ethanol, and water. Having been cleaned, the wafers were etched with a hydrofluoric acid solution (10%) for about 2 min and then rinsed with a large amount of water. The silicon wafers were put into a bath containing the solution of concentrated H_2SO_4:H_2O_2 (v/v 7:3) at 90 °C for several hours and then were washed thoroughly with water. The wafers were dried in a nitrogen (N_2) stream.
(32) He, C.; Sun, J.; Deng, C.; Zhao, T.; Deng, M.; Chen, X.; Jing, X. *Biomacromolecules* **2004**, *5*, 2042.
(33) Hwang, M. J.; Suh, J. M.; Bae, Y. H.; Kim, S. W.; Jeong, B. *Biomacromolecules* **2005**, *6*, 885.
(34) Luo, L.; Tam, J.; Maysinger, D.; Eisenberg, A. *Bioconjugate Chem.* **2002**, *13*, 1259.
(35) Seo, S. H.; Chang, J. Y.; Tew, G. N. *Angew. Chem., Int. Ed.* **2006**, *45*, 7526.
(36) LaRue, I.; Adam, M.; Pitsikalis, M.; Hadjichristidis, N.; Rubinstein, M.; Sheiko, S. S. *Macromolecules* **2006**, *39*, 309.

MA0707234